Optimal Design of Split Partial Second Pass Reverse Osmosis Network for Desalination Applications

Yousef Saif and Ali Almansoori
Dept. of Chemical Engineering, Petroleum Institute, Abu Dhabi, U.A.E

Ali Elkamel
Dept. of Chemical Engineering, University of Waterloo, Waterloo, Canada N2L 3G1

DOI 10.1002/aic.14271
Published online November 8, 2013 in Wiley Online Library (wileyonlinelibrary.com)

Reverse osmosis (RO) network design problem is presented in this study for seawater desalination. The RO pressure vessel is multiple spiral wound modules connected in series. We exploit in this study the RO pressure vessel operation by considering stream property variations within the pressure vessel itself. The design problem allows extraction of high-quality permeates from different locations along the pressure vessel length. Superstructure optimization is adopted to model the RO network in order to find: (1) optimal arrangement of the process units, (2) optimal permeate extraction locations, and (3) production of several permeate streams with different qualities. Several case studies are presented to show the applications of the proposed mathematical programming model. In general, lower treatment cost and higher permeate recovery can be achieved by allowing permeate extraction streams from the RO pressure vessels. *AIChE J*, 60: 520–532, 2014
Keywords: membrane separations, mathematical modeling, process synthesis

Introduction

Seawater desalination by reverse osmosis (RO) is the dominant proven technology beside multistage flash distillation. The primary driving force for the separation is a pressure difference across semipermeable and selective membrane to separate seawater feed stream into lean permeate and concentrated streams. In order to facilitate the separation, high-pressure pumps (HPPs) are used to pressurize the feed streams prior to RO stages. Energy extraction from HPPs by pressure exchangers (PEs) serve to minimize the energy consumption in RO plants. Spiral wound RO module configuration is an attractive option for desalination applications due to their ease of operation, compact density, and fouling control on a commercial scale.[1]

A spiral wound module consists of several flat sheet membranes folded around a central permeate tube. High pressure seawater stream is normally fed into a pressure vessel with a number of RO membrane modules (i.e., around eight elements) connected in a series configuration. In the first module, water permeates through the membrane resulting in permeate and reject streams. This process continues in the subsequent modules with further treatment of the high pressure reject stream and collection of the permeate stream. Typically, the first pass of an RO stage is followed by other RO stages to either further process the high reject stream or to refine the first pass permeate stream. These stages are arranged to process different intermediate streams in order to reach high quality permeate products.[2]

The optimization of RO network problem has been addressed by many research studies to look for optimal sizes and configuration of process units, and their optimal operation. This problem was modeled through a graphical technique to solve for two stage RO network as straight through and tapered arrangements.[3] Another hierarchical two stage procedure was proposed for the RO network design. In the first level, the membrane characteristics and product constraints can be determined, whereas a second level identifies the RO network typology and its operating conditions for desalination applications.[4]

Superstructure optimization of membrane networks has received immense interest in recent years.[5–7] The approach gives rich stream assignments between fresh feed streams, unit operations, and product streams. Based on the graphical representation of the design problem, a mixed integer nonlinear programming model can be formulated to model large design alternatives. The solution of the mathematical programming model eventually provides optimal unit operation arrangement and stream assignments among the unit operations to reach final products from a set of feed streams. A first attempt to model the RO network through superstructure optimization was tackled through the state space approach.[8] An improvement of the RO network model was proposed to give more process network alternatives with a heuristic search and global search algorithms.[9–11] Further analysis of two stage RO network design problem for seawater and brackish water treatment took into account the RO module dimensions as decision variables.[12]

Correspondence concerning this article should be addressed to Y. Saif at yalmohairi@pi.ac.ae.

RO network design problem is assumed to have two RO stages to reach final permeate products with total dissolved salt (TDS) less than 500 ppm. Sensitivity analysis of different feed seawater streams and salt concentrations were analyzed to check how the RO network topology behaves in order to reach different permeate property constraints (i.e., different permeate flow rates and TDS concentrations). These conditions were studied through a superstructure[13,14] by adopting the state space approach.[8] A third RO stage may be required to reach strict permeate qualities (e.g., TDS less than 100 ppm).

RO membrane performance usually declines over time as a result of reversible and irreversible fouling. Consequently, membrane cleaning is a mandatory task to recover the membrane performance due to fouling matter attachment on the membrane surface in the case of reversible fouling conditions. Irreversible fouling leads to membrane structural modification over time which imposes membrane replacement requirements. Several optimization studies were proposed to provide decisions about optimal membrane cleaning and replacement as a function of time-dependent permeability coefficient decline.[15–17]

The previous design optimization problems consider the RO pressure vessel as an input of only a single-feed stream and two output product streams (e.g., concentrated and permeate streams). Split partial second pass reverse osmosis (SPSPRO) design concept is a novel design compared with other RO design problems. In the SPSPRO design, permeate streams are extracted at different locations along the length of the pressure vessels. This design concept allows the production of different grades of permeate streams from a single-pressure vessel which provides flexibility in the operation of RO plants.[2,18–20]

In this study, we consider the SPSPRO design concept through superstructure optimization for desalination applications. The design problem will be presented as to process seawater feed stream by RO units in different stages. Utility units (pumps and PEs) will serve the purpose of delivering and recovering energy from different streams. These unit operations will be linked through rich combinations by a superstructure representation. Mixed integer nonlinear programming model will be developed based on the superstructure representation to evaluate large process network alternatives simultaneously. In the following sections, design concept preliminaries will be given to shed light on important aspects of the SPSPRO network design problem and to define the problem statement. Further, we will explain the superstructure representation, followed by the mathematical programming formulation. Case studies will be given to illustrate the advantages of the proposed SPSPRO design problem. Finally, we give the conclusions from the research study.

SPSPRO Design Problem

It is appropriate at this point to define some important terms before discussing the SPSPRO network. A RO module or element is composed of several RO flat sheet membranes folded around a central permeate tube (e.g., spiral wound module). These modules are connected in a series arrangement within a high-pressure vessel. A RO stage or a pass is composed of several number of high-pressure vessels operating under the same conditions of flow rate, pressure, and chemical composition. The RO network design problem under consideration will have several RO stages, pumps, and energy recovery units such as PEs. Figure 1 depicts the unit operations that may exist in every RO stage.

Process synthesis problems exploit stream properties and manipulate them by mixing, splitting, and unit operations to reach the desired final products through a superstructure representation. Likewise, it is important to exploit the stream properties inside the unit operations. The essential driving force for an RO unit is a pressure difference across the membrane. This driving force deteriorates along the length of the pressure vessel due to the increase of TDS concentration and increase of the osmotic pressure. A good RO module design should minimize the pressure drop in order to act against the increase of osmotic pressure and optimize the operating conditions.

During the operation of an RO pressure vessel, the first RO modules normally produce higher flow rate of permeate with lower TDS compared with the last modules, Figures 2 and 3. One can notice that the detailed knowledge of flow rate and TDS distribution within pressure vessel is an important factor if the production of different permeate grades is desirable. In the SPSPRO design concept, different permeate streams are extracted from the pressure vessel and directed either to another pass for further processing or to the final product collection points.[2,18–20]

This study considers permeate stream side extraction from every RO module existing within the pressure vessels in the RO network design problem. The RO design approach allows meeting strict final permeate streams with high qualities as a result of high quality permeate stream extraction from the front modules. In the case of meeting higher quality permeate streams that cannot be met from the first pass, a second RO stage can further process the first pass permeate streams to reach the final demand product constraints. An

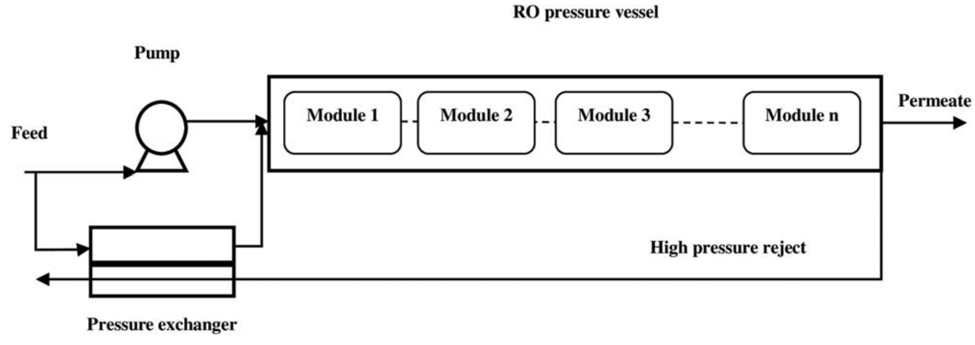

Figure 1. RO stage with auxiliary equipments.

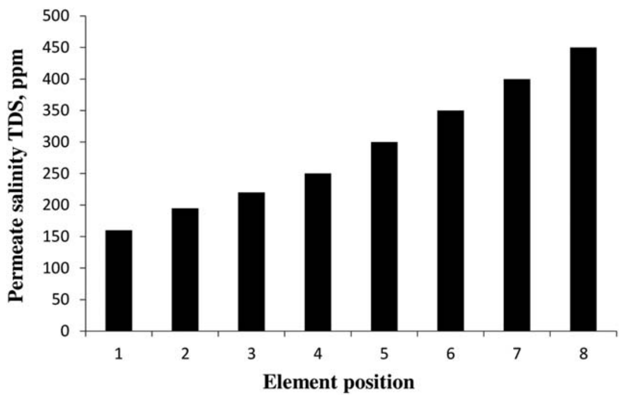

Figure 2. Permeate salinity along the pressure vessel length.[2]

RO stage can be represented by Figure 4 to illustrate permeate stream withdrawals and the utility units (pumps and PEs). Clearly, the problem requires a systematic engineering approach in order to give an optimal solution for the SPSPRO layout.

The design problem can be addressed as given below:

- seawater stream with known TDS concentration;
- set of RO membranes with different TDS rejection characteristics (MEMB);
- set of RO stages (SRO);
- set of pump units (HPP);
- set of booster pumps (BP);
- set of pressure exchanger units (PE).

The task is to synthesize an SPSPRO treatment plant to meet several permeate streams with different qualities. To give answers for the previous problem, a superstructure representation of the design problem is necessary to develop a mathematical programming model. The next section explains the superstructure representation in this research study.

RO Network Superstructure

RO superstructure represents different process layouts or alternatives to give a designer an assortment of alternatives for simultaneous evaluation. This study gives compact representation for the process units in every RO stage. In general, every stage has sets of mixer and splitter nodes. The mixer nodes are the points for mixing streams from different stages to provide RO feed streams, whereas the splitter nodes split the RO stage product streams to other RO stages and to the final product mixer nodes.

Figure 5 is another way of representing an RO stage compared with Figure 4. The first mixer (MIX1) is a feed stream which will be processed by the RO stage. This stream results from mixing different streams coming from other RO stages. In order to raise the feed pressure, the stream can be directed to a HPP. Also, this stream can be split partially to the PE unit and followed by a BP to match the HPP exit stream. Another mixer (MIX2) receives a high-pressure stream which is a feed stream to the PE unit. This node serves the purpose of extracting kinetic energy in the PE unit from other RO stages.

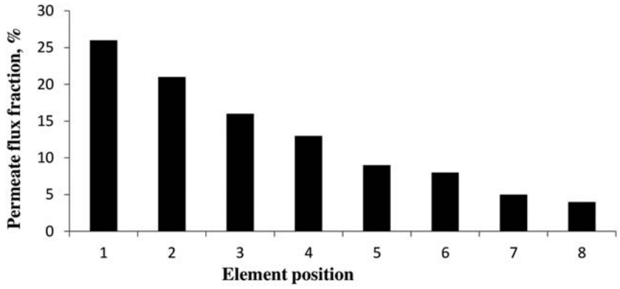

Figure 3. Flux distribution in eight element RO pressure vessel.[2]

The splitter nodes act as other venues of interactions between different RO stages. These splitter nodes (SP_1-SP_n) provide locations for permeate extraction. After the splitter nodes, permeate streams with different qualities can be directed to the final product permeate streams and other RO stages. The splitter SP_{n+1} is the high pressure reject splitter coming out of the RO stage. This node acts as a source of interaction with other RO stages, other PEs, and the final reject streams going out of the network. The last splitter SP_{n+2} has an exhausted stream coming out of the PE unit which flows out of the network. It should be emphasized that the energy recovered in the PE may not match the HPP exit stream conditions. In this case, a BP is needed to raise the pressure to the HPP exit stream conditions.

The superstructure of SPSPRO network can be assembled through the given input information of seawater TDS concentration, set of RO stages, and the final permeate product stream demand. The set of any RO stage is composed of parallel RO pressure vessels which house several number of RO modules connected in series. Any RO feed stream is split equally over all the RO pressure vessels in the RO stage. Besides, HPP, BP, and PE units supplement the RO stage operation requirements as explained in Figure 4. The SPSPRO superstructure representation is depicted by Figure 6. It shows the stream distribution for the SPSPRO network from the inlet seawater feed until the final permeate products for two RO stages. It is worth pointing out that the representation can be assembled for any number of RO stages following the same concept of Figure 6.

The inlet feed seawater stream is distributed over the RO stages (SRO) in the distribution box (DB). These stream assignments link the inlet seawater feed to the mixer nodes for every RO stage. The exit streams from every RO stage (i.e., streams from the splitter SP_1 to SP_{n+2}) enter the DB as feed streams to the RO stages and the final reject and permeate streams. This representation gives rich stream assignments between the inlet seawater feed stream, RO stages, and the final reject and permeate streams. Within this network, a designer looks for an optimal SPSPRO layout to treat the feed seawater stream and to reach the final permeate product constraints. The given SPSPRO network has some analogy with distillation network representation taking into account side stream extractions from different locations along the length of a distillation column.[21–23] The next section gives the mathematical programming formulation for the SPSPRO network model.

Mathematical Programming Model

The mathematical programming model formulation for the SPSPRO network is a mixed integer nonlinear program (MINLP). The discrete variables model the selection of membrane types in every RO module, the existence of RO modules, the existence of auxiliary equipments, and the stream assignments in the DB. All other variables are

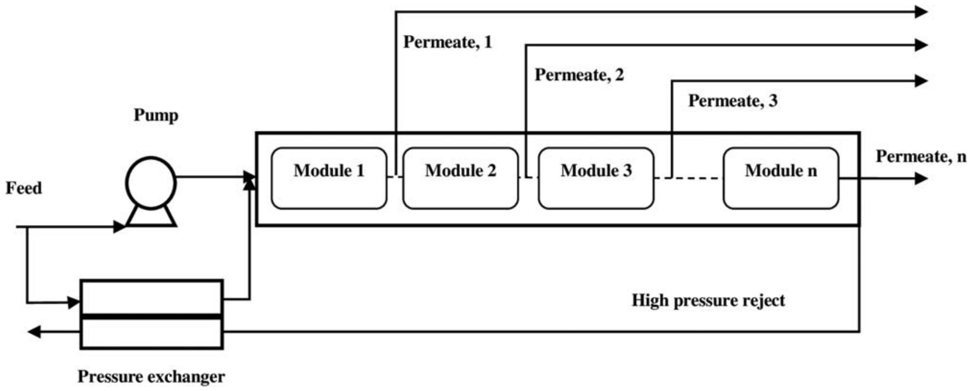

Figure 4. SPSPRO stage with auxiliary equipments.

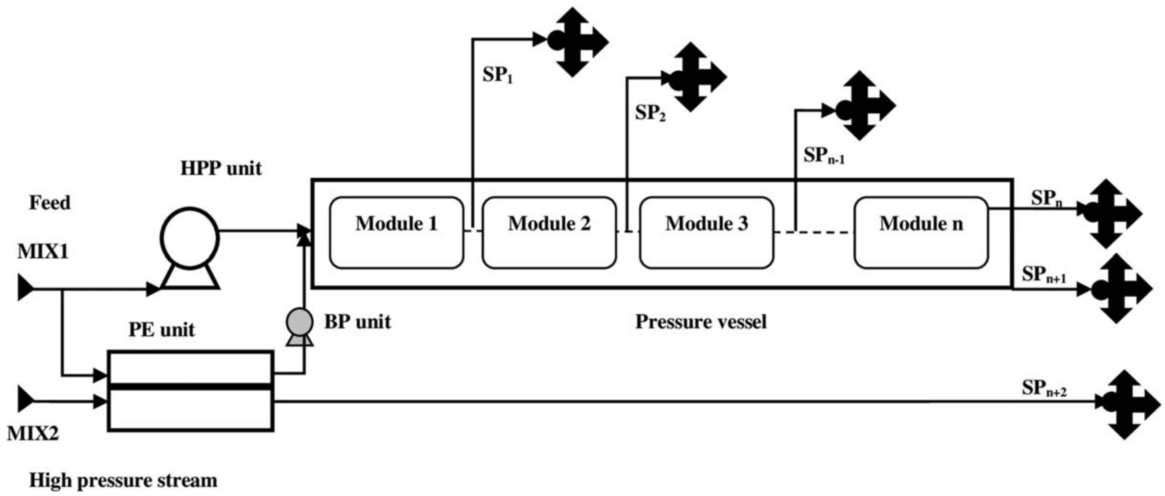

Figure 5. Splitter and mixer nodes representation for an RO stage with auxiliary equipments.

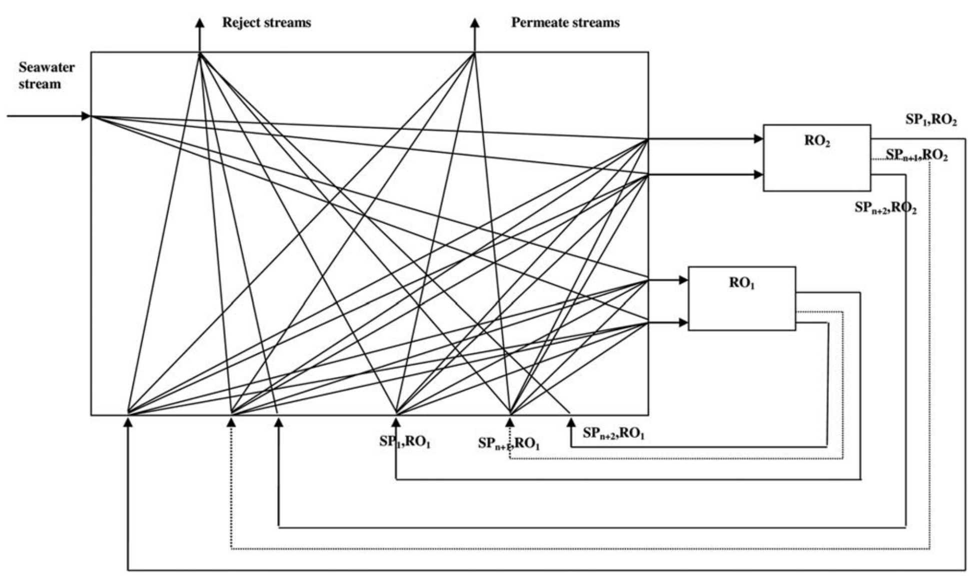

Figure 6. Split partial second pass RO superstructure representation for two RO stages.

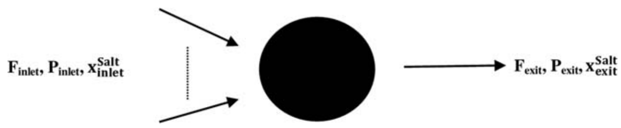

Figure 7. A mixer node representing input flow streams and a single-product stream.

continuous such as flow, pressure, and concentration. In the DB, there are many mixer and splitter nodes to allow interactions between different stream states in the network. A mixer node is given by Figure 7 which shows different streams going through the node to yield an input feed for an RO stage or the final product streams. The mixer node requires total and component balances as given by Eqs. 1 and 2.

$$F_{\text{exit}} = \sum^{\text{inlet}} F_{\text{inlet}} \quad \forall \text{exit}. \tag{1}$$

$$F_{\text{exit}} x^{\text{Salt}}_{\text{exit}} = \sum^{\text{inlet}} F_{\text{inlet}} x^{\text{Salt}}_{\text{inlet}} \quad \forall \text{exit}. \tag{2}$$

A restriction of mixing the input streams is limited to only streams with equivalent pressure values as

$$F_{\text{inlet}} \leq F^{\text{UP}}\, y_{\text{inlet,exit}} \; \forall \text{inlet, exit} \tag{3}$$

$$P_{\text{exit}} - P_{\text{inlet}} \leq P^{\text{UP}}\, (1 - y_{\text{inlet,exit}}) \; \forall \text{inlet, exit} \tag{4}$$

$$P_{\text{exit}} - P_{\text{inlet}} \geq P^{\text{LO}}\, (1 - y_{\text{inlet,exit}}) \; \forall \text{inlet, exit} \tag{5}$$

where $y_{\text{inlet,exit}}$ is a binary variable to allow mixing between every inlet stream and the mixer product stream. The set of Eqs. 3–5 forces the input streams to diminish if there is no pressure match with the mixer exit stream.

A splitter node has an opposite action compared with the mixer node, Figure 8. A single-feed stream is split into several streams with the same properties as given by Eq. 6. These exit streams will be mixed with other splitter output streams to have conditions matching a mixer node exit conditions as explained before by Eqs. 3–5.

$$F_{\text{inlet}} = \sum^{\text{exit}} F_{\text{exit}} \tag{6}$$

There are restrictions for the final permeate product streams on the flow rate (F_{PERMEATE}) and TDS concentration ($x^{\text{Salt}}_{\text{PERMEATE}}$) demand through the following equations.

$$F_{\text{PERMEATE}} \geq F^{\text{LO}}_{\text{PERMEATE}} \; \forall \, \text{PERMEATE} \tag{7}$$

$$x^{\text{salt}}_{\text{PERMEATE}} \leq x^{\text{UP,Salt}} \; \forall \, \text{PERMEATE} \tag{8}$$

The RO stage set (SRO) will have a set of governing equations describing the transport of water mass flow rate, $F^{\text{Wat}}_{\text{Elem,RO}}$, and salt mass flow rate, $F^{\text{Salt}}_{\text{Elem,RO}}$, across the membrane for every module. This model follows the solution diffusion model.[13,15,24] It assumes negligible effects of the channel curvature as the feed channel thickness is much lower than the RO module radius. Further, the permeate channel pressure drop is not significant. The concentration polarization is modeled by the film theory. In addition, it is assumed that the RO membrane performs under clean conditions (e.g., no fouling effects). The water mass flow rate and the salt transfer across the membrane are described by the following equations

$$\begin{aligned} F^{\text{Wat}}_{\text{Elem,RO}} = {} & \text{SA}_{\text{Elem,RO}}\, \text{Wa}_{\text{Elem,RO}} \Big(P^{\text{REJ,in}}_{\text{Elem,RO}} - \Delta P_{\text{Elem,RO}} \\ & - P^{\text{PERM}}_{\text{Elem,RO}} - \big(\pi^{\text{REJ}}_{\text{Elem,RO}} - \pi^{\text{PERM}}_{\text{Elem,RO}} \big) \Big) \\ & \forall\, \text{Elem, RO} \in \text{SRO} \end{aligned} \tag{9}$$

$$\begin{aligned} F^{\text{Salt}}_{\text{Elem,RO}} = {} & \text{SA}_{\text{Elem,RO}}\, B_{\text{Elem,RO}}\, (x^{\text{R-Wall}}_{\text{Elem,RO}} - x^{\text{P-Wall}}_{\text{Elem,RO}}) \\ & \forall\, \text{Elem, RO} \in \text{SRO} \end{aligned} \tag{10}$$

$\text{SA}_{\text{Elem,RO}}$ is the effective membrane surface area for every module. $\text{Wa}_{\text{Elem,RO}}$, and $B_{\text{Elem,RO}}$ represent the water and salt permeability coefficients, respectively. $P^{\text{REJ,in}}_{\text{Elem,RO}}$, $\Delta P_{\text{Elem,RO}}$, and $P^{\text{PERM}}_{\text{Elem,RO}}$ are the inlet reject pressure, pressure drop, and permeate pressure in the RO module, respectively. The osmotic pressure in the reject and permeate sides are given by $\pi^{\text{REJ}}_{\text{Elem,RO}}$, and $\pi^{\text{PERM}}_{\text{Elem,RO}}$, where $x^{\text{R-Wall}}_{\text{Elem,RO}}$ and $x^{\text{P-Wall}}_{\text{Elem,RO}}$ are the salt concentration at the reject and permeate membrane wall, respectively.

The osmotic pressure at the reject ($\pi^{\text{REJ}}_{\text{Elem,RO}}$) and permeate sides ($\pi^{\text{PERM}}_{\text{Elem,RO}}$) are correlated with the salt concentration at the membrane wall as given by Eqs. 11 and 12. The seawater property correlations found in the literature are nonlinear functions of seawater TDS concentration and temperature.[25,26] Nonetheless, the proposed seawater property correlations (e.g., osmotic pressure, density, and viscosity) were found to behave as linear functions of TDS concentration under the range covered in this study assuming RO isothermal condition. These linear correlations were obtained by simulation of nonlinear models and curve fitting the generated data with R^2 higher than 99%. $x^{\text{R-Wall}}_{\text{Elem,RO}}$ and $x^{\text{P-Wall}}_{\text{Elem,RO}}$ are the TDS concentration at the membrane wall for the reject and permeate sides. It can be seen from Eq. 9 that the osmotic pressure at the reject side will reduce the water flow across the membrane, whereas the osmotic pressure at the permeate side has an opposite effect.

$$\pi^{\text{REJ}}_{\text{Elem,RO}} = 70 + 0.1716\, x^{\text{R-Wall}}_{\text{Elem,RO}} \; \forall\, \text{Elem, RO} \in \text{SRO} \tag{11}$$

$$\pi^{\text{PERM}}_{\text{Elem,RO}} = 70 + 0.1716\, x^{\text{P-Wall}}_{\text{Elem,RO}} \; \forall\, \text{Elem, RO} \in \text{SRO} \tag{12}$$

The concentration polarization describes the transport of salt at the reject side by Eq. 13. The mass transfer ($k_{\text{Elem,RO}}$), permeate velocity ($V_{\text{Elem,RO}}$), and permeate concentration at membrane wall are given by Eqs. 14–16, respectively. These equations assume a fully developed concentration polarization layer on the RO membrane surface.

$$\begin{aligned} x^{\text{R-Wall}}_{\text{Elem,RO}} = {} & x^{\text{P-Wall}}_{\text{Elem,RO}} + \left(\frac{x^{\text{REJ},f}_{\text{Elem,RO}} + x^{\text{REJ,bulk}}_{\text{Elem,RO}}}{2} - x^{\text{P-Wall}}_{\text{Elem,RO}} \right) e^{\frac{V_{\text{Elem,RO}}}{k_{\text{Elem,RO}}}} \\ & \forall\, \text{Elem, RO} \in \text{SRO} \end{aligned} \tag{13}$$

$$\begin{aligned} k_{\text{Elem,RO}} = {} & 0.04\, \text{Re}^{0.75}_{\text{Elem,RO}}\, \text{Sc}^{0.33}_{\text{Elem,RO}}\, \frac{D^{\text{Salt}}_{\text{Elem,RO}}}{d} \\ & \forall\, \text{Elem, RO} \in \text{SRO} \end{aligned} \tag{14}$$

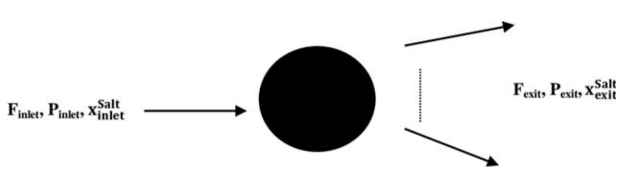

Figure 8. A splitter node representing an input flow stream and output product streams.

$$V_{\text{Elem,RO}} = \frac{F^{\text{Wat}}_{\text{Elem,RO}} + F^{\text{Salt}}_{\text{Elem,RO}}}{\text{SA}_{\text{Elem,RO}}\ \rho^{\text{PERM}}_{\text{Elem,RO}}}\ \forall\,\text{Elem},\text{RO} \in \text{SRO} \tag{15}$$

$$x^{\text{PERM}}_{\text{Elem,RO}} = \frac{F^{\text{Salt}}_{\text{Elem,RO}}}{F^{\text{Wat}}_{\text{Elem,RO}} + F^{\text{Salt}}_{\text{Elem,RO}}}\ \forall\text{Elem},\text{RO} \in \text{SRO} \tag{16}$$

$x^{\text{REJ}\,f}_{\text{Elem,RO}}$ and $x^{\text{REJ,bulk}}_{\text{Elem,RO}}$ are the feed and bulk salt concentration at the reject side. $\text{Re}_{\text{Elem,RO}}$, $\text{Sc}_{\text{Elem,RO}}$, $D^{\text{Salt}}_{\text{Elem,RO}}$, and d are Reynold's, Schmidt, salt diffusivity, and feed space thickness, respectively. The permeate density ($\rho^{\text{PERM}}_{\text{Elem,RO}}$) and reject density ($\rho^{\text{REJ}}_{\text{Elem,RO}}$) are function of the RO module average TDS concentration as given by the following equations.

$$\rho^{\text{PERM}}_{\text{Elem,RO}} = 700\,x^{\text{P-avg}}_{\text{Elem,RO}} + 998\ \forall\,\text{Elem},\text{RO} \in \text{SRO} \tag{17}$$

$$\rho^{\text{REJ}}_{\text{Elem,RO}} = 700\,x^{\text{R-avg}}_{\text{Elem,RO}} + 998\ \forall\,\text{Elem},\text{RO} \in \text{SRO} \tag{18}$$

The reject flow exhibits pressure drop ($\Delta P^{\text{REJ}}_{\text{Elem,RO}}$) for every element as given by Eq. 19.

$$\Delta P^{\text{REJ}}_{\text{Elem,RO}} = \left(\frac{9.2\times10^{-13}\,Q_{\text{Elem,RO}}\,L_{\text{Elem,RO}}\,\mu_{\text{Elem,RO}}}{W\,d^3}\right)\quad \forall\,\text{Elem},\text{RO} \in \text{SRO} \tag{19}$$

$Q_{\text{Elem,RO}}$, $L_{\text{Elem,RO}}$, $\mu_{\text{Elem,RO}}$, and W are the average volumetric flow rate at the reject side, length of membrane element, reject viscosity, and membrane element width, respectively. The reject viscosity is approximated by Eq. 20 as a linear function of the average reject salt concentration ($x^{\text{R-avg}}_{\text{Elem,RO}}$) similar to the other seawater properties.

$$\mu^{\text{REJ}}_{\text{Elem,RO}} = 2\times10^{-3}\,x^{\text{R-avg}}_{\text{Elem,RO}} + 0.0009\ \forall\,\text{Elem},\text{RO} \in \text{SRO} \tag{20}$$

The mass change on the reject side is equivalent to the permeate mass change for every element as given by Eq. 21.

$$F^{\text{REJ,in}}_{\text{Elem,RO}} - F^{\text{REJ,out}}_{\text{Elem,RO}} = F^{\text{PERM,out}}_{\text{Elem,RO}} - F^{\text{PERM,in}}_{\text{Elem,RO}}\ \forall\text{Elem},\text{RO} \in \text{SRO} \tag{21}$$

Besides, the salt balance on the reject and permeate sides can be calculated by the following equations.

$$F^{\text{REJ,in}}_{\text{Elem,in,RO}}\ x^{\text{REJ,in,Salt}}_{\text{Elem,RO}} - F^{\text{REJ,out}}_{\text{Elem,RO}}\ x^{\text{REJ,out,Salt}}_{\text{Elem,RO}} = F^{\text{Salt}}_{\text{Elem,RO}}\quad \forall\,\text{Elem},\text{RO} \in \text{SRO} \tag{22}$$

$$F^{\text{PERM,in}}_{\text{Elem,RO}}\ x^{\text{PERM,in,Salt}}_{\text{Elem,RO}} + F^{\text{Salt}}_{\text{Elem,RO}} = F^{\text{PERM,out}}_{\text{Elem,RO}}\ x^{\text{PERM,out,Salt}}_{\text{Elem,RO}}\quad \forall\,\text{Elem},\text{RO} \in \text{SRO} \tag{23}$$

The reject stream flows from one element to the next one which requires balance equations for the flow, pressure, and salt concentration, Eqs. 24–26.

$$F^{\text{REJ,in}}_{\text{Elem}+1,\text{RO}} = F^{\text{REJ,out}}_{\text{Elem,RO}}\ \forall\,\text{Elem},\text{RO} \in \text{SRO} \tag{24}$$

$$x^{\text{REJ,in,Salt}}_{\text{Elem}+1,\text{RO}} = x^{\text{REJ,out,Salt}}_{\text{Elem,RO}}\ \forall\,\text{Elem},\text{RO} \in \text{SRO} \tag{25}$$

$$P^{\text{REJ,in}}_{\text{Elem}+1,\text{RO}} = P^{\text{REJ,out}}_{\text{Elem,RO}}\ \forall\,\text{Elem},\text{RO} \in \text{SRO} \tag{26}$$

On the permeate side, withdraw streams exist between any adjacent element which require total balance as given by Eq. 27. The withdrawal stream and the incoming stream to the next element keep the same pressure and salt concentration from the previous element.

$$F^{\text{PERM,out}}_{\text{Elem,RO}} = F^{\text{PERM,in}}_{\text{Elem}+1,\text{RO}} + F^{\text{WITHD}}_{\text{Elem,RO}}\ \forall\,\text{Elem},\text{RO} \in \text{SRO} \tag{27}$$

The overall SPSPRO stage flow rate is linked to the pressure vessel equation by the total number of pressure vessel existing in that stage, Eq. 28.

$$F^{\text{in}}_{\text{RO}} = F^{\text{REJ,in}}_{\text{Elem}=1,\text{RO}}\ \text{NPV}_{\text{RO}}\ \forall\,\text{RO} \in \text{SRO} \tag{28}$$

Similarly, the permeate withdraw stream from every element and the total reject side in every stage is described by Eqs. 29 and 30.

$$F^{\text{REJ}}_{\text{RO}} = F^{\text{REJ,out}}_{\text{Elem}=n,\text{RO}}\ \text{NPV}_{\text{RO}}\ \forall\,\text{RO} \in \text{SRO} \tag{29}$$

$$F^{\text{WITHD}-\text{Total}}_{\text{Elem,RO}} = F^{\text{WITHD}}_{\text{Elem,RO}}\ \text{NPV}_{\text{RO}}\ \forall\,\text{RO} \in \text{SRO} \tag{30}$$

In addition, the exit pressure and concentration from the last element on the reject side give the exit condition for the reject side in that stage. It is worth pointing out that the set of Eqs. 9–30 describe the nonlinear behavior of the SPSPRO stage.

The existence of any RO element is related to a binary variable ($y_{\text{Elem,RO}}$) to indicate if there is transport of mass (water and salt) across the membrane as described by Eq. 31.

$$F^{\text{Wat}}_{\text{Elem,RO}} + F^{\text{Salt}}_{\text{Elem,RO}} \le F^{\text{UP}}_{\text{Elem,RO}}\ y_{\text{Elem,RO}}\ \forall\,\text{Elem},\text{RO} \in \text{SRO} \tag{31}$$

The RO stage existence is a relation between the first element binary variable in the RO stage with the stage inlet flow, Eq. 32.

$$F^{\text{in}}_{\text{RO}} \le F^{\text{REJ,UP,in}}_{\text{Elem}=1,\text{RO}}\ \text{NPV}^{\text{UP}}_{\text{RO}}\ y_{\text{Elem}=1,\text{RO}}\ \forall\,\text{RO} \in \text{SRO} \tag{32}$$

Every element has a membrane that can be selected from a membrane set (MEMB) following the relation given by Eq. 33.

$$\sum^{\text{Memb}} y_{\text{Memb,Elem,RO}} \le 1\ \forall\,\text{Elem},\text{RO} \in \text{SRO} \tag{33}$$

The previous relation forces the search procedure to select only one optimal membrane type with respect to the states present inside the RO module in every RO stage. It may not be appropriate to select different types of membranes for consecutive elements in a single stage. Equation 34 is a relation to select only one membrane type in every RO stage.

$$y_{\text{Memb,Elem}-1,\text{RO}} \ge y_{\text{Memb,Elem,RO}}\ \forall\,\text{MEMB},\ \text{Elem}>1,\ \text{RO} \in \text{SRO} \tag{34}$$

Consequently, water and salt permeability coefficients ($Wa_{\text{Elem,RO}}$, $B_{\text{Elem,RO}}$), and the surface area ($\text{SA}_{\text{Elem,RO}}$) have the same values in every element present in the pressure vessels, Eqs. 35–37.

$$Wa_{\text{Elem,RO}} = \sum^{\text{Memb}} Wa_{\text{Memb,Elem,RO}}\ y_{\text{Memb,Elem,RO}}\quad \forall\text{Elem},\ \text{RO} \in \text{SRO} \tag{35}$$

$$B_{\text{Elem,RO}} = \sum^{\text{Memb}} B_{\text{Memb,Elem,RO}}\ y_{\text{Memb,Elem,RO}}\quad \forall\text{Elem},\ \text{RO} \in \text{SRO} \tag{36}$$

$$\mathrm{SA}_{\mathrm{Elem,RO}} = \sum^{\mathrm{Memb}} \mathrm{SA}_{\mathrm{Memb,Elem,RO}}\, y_{\mathrm{Memb,Elem,RO}} \quad \forall \mathrm{Elem},\ \mathrm{RO} \in \mathrm{SRO} \tag{37}$$

where $W_{\mathrm{Memb,Elem,RO}}$, $B_{\mathrm{Memb,Elem,RO}}$, and $\mathrm{SA}_{\mathrm{Memb,Elem,RO}}$ represent water and salt permeability coefficients, and the surface area for every membrane type. It should be noted that different membrane type imposes different feed flow rate and pressure conditions as shown by the following equations.

$$F^{\mathrm{REJ,in}}_{\mathrm{Elem,RO}} \le F^{\mathrm{UP}}_{\mathrm{Memb}}\, y_{\mathrm{Memb,Elem,RO}} + F^{\mathrm{UP}}\,(1 - y_{\mathrm{Memb,Elem,RO}}) \quad \forall \mathrm{Memb,Elem,RO} \in \mathrm{SRO} \tag{38}$$

$$F^{\mathrm{REJ,in}}_{\mathrm{Elem,RO}} \ge F^{\mathrm{LO}}_{\mathrm{Memb}}\, y_{\mathrm{Memb,Elem,RO}} \quad \forall \mathrm{Memb,Elem,RO} \in \mathrm{SRO} \tag{39}$$

$$P^{\mathrm{REJ,in}}_{\mathrm{Elem,RO}} \le P^{\mathrm{UP}}_{\mathrm{Memb}}\, y_{\mathrm{Memb,Elem,RO}} + P^{\mathrm{UP}}\,(1 - y_{\mathrm{Memb,Elem,RO}}) \quad \forall \mathrm{Memb,Elem,RO} \in \mathrm{SRO} \tag{40}$$

The first terms on the right of the inequalities of Eqs. 38 and 40 force the flow and pressure feed inlet conditions to have upper values suitable for the selected membrane type, whereas the second terms relax the constraints for the other case. Equation 39 maintains a minimum flow in the RO element.

The existence of the auxiliary equipments (HPP, BP, and PEs) is a relation between the pressure difference across the unit operation and its binary variable as given by the following equations.

$$P^{\mathrm{out}}_{\mathrm{HPP}} - P^{\mathrm{in}}_{\mathrm{HPP}} \le P^{\mathrm{UP}}\, y_{\mathrm{HPP}} \quad \forall \mathrm{HPP} \tag{41}$$

$$P^{\mathrm{out}}_{\mathrm{BP}} - P^{\mathrm{in}}_{\mathrm{BP}} \le P^{\mathrm{UP}}\, y_{\mathrm{BP}} \quad \forall \mathrm{BP} \tag{42}$$

$$P^{\mathrm{out}}_{\mathrm{PE}} - P^{\mathrm{in}}_{\mathrm{PE}} \le P^{\mathrm{UP}}\, y_{\mathrm{PE}} \quad \forall \mathrm{PE} \tag{43}$$

In this model, the constraint set 1–43 defines nonconvex feasible region of the MINLP. The objective function in this study minimizes the total annual cost (TAC) for the treatment of seawater stream given in the abovementioned constraints.

The total capital cost is composed of pressure vessels and membrane type costs, seawater intake pump and feed pretreatment, high pressure and BPs, and the PE units as given by Eqs. 44–49 with a practical investment factor (PIF) reflecting the indirect capital cost as a percentage of total capital cost.[27] The operating cost has electricity operational cost for the RO pressure vessel, seawater intake pump, HPP, PE units, Eqs. 50–53. Other operational cost includes insurance, labor, chemical usage, and maintenance for the RO plant, Eqs. 54–57. The estimated TAC is given by Eq. 59 assuming annual interest rate of 5% and plant lifetime set at 25 years.[13]

$$\mathrm{CC}_{\mathrm{PV}} = \sum^{\mathrm{Memb}} \sum^{\mathrm{Elem}} \sum^{\mathrm{ROS}} C_{\mathrm{Memb}}\, y_{\mathrm{Memb,Elem,RO}}\, \mathrm{NPV}_{\mathrm{RO}} + \sum^{\mathrm{ROS}} C_{\mathrm{PV}}\, \mathrm{NPV}_{\mathrm{RO}} \tag{44}$$

$$\mathrm{CC}_{\mathrm{SWIP}} = C_{\mathrm{SWIP}}\,(F_{\mathrm{SWIP}})^{n_1} \tag{45}$$

$$\mathrm{CC}_{\mathrm{HPP}} = C_{\mathrm{HPP}}\,(F_{\mathrm{HPP}}\,\Delta P_{\mathrm{HPP}}) \tag{46}$$

$$\mathrm{CC}_{\mathrm{BP}} = C_{\mathrm{BP}}\,(F_{\mathrm{BP}}\,\Delta P_{\mathrm{BP}}) \tag{47}$$

$$\mathrm{CC}_{\mathrm{PE}} = C_{\mathrm{PE}}\,(F^{\mathrm{HI}}_{\mathrm{PE}})^{n_2} \tag{48}$$

$$\mathrm{TCC} = \mathrm{PIF}\,(\mathrm{CC}_{\mathrm{PV}} + \mathrm{CC}_{\mathrm{SWIP}} + \mathrm{CC}_{\mathrm{HPP}} + \mathrm{CC}_{\mathrm{BP}} + \mathrm{CC}_{\mathrm{PE}}) \tag{49}$$

$$\mathrm{OC}_{\mathrm{PV}} = \mathrm{O}_{\mathrm{PV}}\, \mathrm{CC}_{\mathrm{PV}} \tag{50}$$

$$\mathrm{OC}_{\mathrm{SWIP}} = O_{\mathrm{SWIP}}\, \frac{F_{\mathrm{SWIP}}}{\eta_{\mathrm{SWIP}}\, \eta_{\mathrm{MOTOR}}} \tag{51}$$

$$\mathrm{OC}_{\mathrm{HPP}} = O_{\mathrm{HPP}}\, \frac{F_{\mathrm{HPP}}\,\Delta P_{\mathrm{HPP}}}{\eta_{\mathrm{HPP}}\, \eta_{\mathrm{MOTOR}}} \tag{52}$$

$$\mathrm{OC}_{\mathrm{PE}} = O_{\mathrm{PE}}\, \frac{F_{\mathrm{PEHI}}\,\Delta P_{\mathrm{PEHI}}}{\eta_{\mathrm{PE}}\, \eta_{\mathrm{MOTOR}}} \tag{53}$$

$$\mathrm{OC}_{\mathrm{INSURANCE}} = O_{\mathrm{INSURANCE}}\, \mathrm{TCC} \tag{54}$$

$$\mathrm{OC}_{\mathrm{LABOR}} = O_{\mathrm{LABOR}} \sum^{\mathrm{FPERM}} F_{\mathrm{FPERM}} \tag{55}$$

$$\mathrm{OC}_{\mathrm{CHEMICAL}} = O_{\mathrm{CHEMICAL}}\, F_{\mathrm{SWIP}} \tag{56}$$

$$\mathrm{OC}_{\mathrm{MAINT}} = O_{\mathrm{MAINT}} \sum^{\mathrm{FPERM}} F_{\mathrm{FPERM}} \tag{57}$$

$$\mathrm{AOC} = \mathrm{OC}_{\mathrm{PV}} + \mathrm{OC}_{\mathrm{SWIP}} + \mathrm{OC}_{\mathrm{HPP}} + \mathrm{OC}_{\mathrm{PE}} + \mathrm{OC}_{\mathrm{INSURANCE}} + \mathrm{OC}_{\mathrm{LABOR}} + \mathrm{OC}_{\mathrm{CHEMICAL}} + \mathrm{OC}_{\mathrm{MAINT}} \tag{58}$$

$$\mathrm{TAC} = \mathrm{AF}\ \mathrm{TCC} + \mathrm{AOC} \tag{59}$$

The mathematical programming model (MINLP) defined by the set of constraints and the objective function TAC has several local optima due to the presence of nonconvex terms. In this study, we applied DICOPT solver[28] in general algebraic modeling system (GAMS)[29] (Brooke et al.) to solve all the case studies. The MINLP decomposition algorithm coded in DICOPT is based on extensions of the outer-approximation algorithm.[30] This code solves successive non-linear programming (NLP) and mixed integer linear programming (MILP) subproblems which converge normally to a local optimal solution based on a good quality starting point. Beside, the algorithm has provisions to manage nonconvex functions that normally arise in design problems. All the case studies will be solved from an exhaustive random search procedure, however, the global solution is not guaranteed. This search procedure generates random starting points for the binary and continuous variables and the convergence is attained if these starting points are close to local optimal solution. There are many local optimal solutions for these case studies and the best local optimal solution is reported for every case study. Next section will cover several case studies with various input seawater feed concentration and different permeate product demand constraints.

Table 1. Characteristics of FilmTec Spiral Wound Reverse Osmosis Membrane Elements

Module Type	SW30XLE-400	SW30HR-380	SW30HR-320	BW30–400
Active area (m^2)	37.2	35.3	29.7	37
Length of the element (m)	0.88	0.88	0.88	0.88
Feed space (m)	8.126×10^{-9}	8.126×10^{-9}	8.126×10^{-9}	8.126×10^{-9}
Feed flow rate range (kg/s)	$4.5 - 0.22$	$4.5 - 0.22$	$3.9 - 0.22$	$5.3 - 0.22$
Max. operating pressure (MPa)	8.3	8.3	8.3	4.5
Water permeability (kg/m^2 s MPa)	3.5×10^{-3}	2.7×10^{-3}	3.1×10^{-3}	7.5×10^{-3}
TDS permeability (kg/m^2 s)	3.2×10^{-5}	2.3×10^{-5}	2.2×10^{-5}	6.2×10^{-5}
Membrane element cost ($)	1200	1000	1400	900

Case Studies

The SPSPRO mathematical programming model will be applied on case studies to investigate potential benefits of splitting permeate streams from the RO pressure vessels. These results will be compared with the same input parameters in the case of no permeate splitting conditions. It should be noted that the optimization problems in every case study has the same constraints and variable dimensions. The optimization problems under nonpermeate extraction condition were solved after setting the flow rate of permeate extracted streams to zero values in the SPSPRO model. The largest optimization problem (case study four) in this research article has 1505 constraints, 1058 variables, and 130 binary variables. The solution time for this case study takes around 8 CPU second with DICOPT solver.

In addition, the case studies will have different seawater feed compositions and final permeate flow rate and concentration demand constraints. The aim of these studies will be the productions of multiple permeate streams. Four types of FilmTec RO membrane elements (SW30XLE-400, SW30HR-380, SW30HR-320, and BW30–400) from Dow will be included as options to operate the RO pressure vessels. The transport characteristics and module geometry for every type considered are given in Table 1. The parameters and cost coefficients used in the optimization model are listed in Table 2.

Table 2. The Parameters and Cost Coefficients for Calculation

Feed water temperature (°C)	25
Diffusion coefficient (m^2/s)	1.493×10^{-9}
High-pressure pump efficiency	75%
n_1	0.8
n_2	0.58
Practical investment factor	1.114
Annualized factor AF, (1/year)	0.08
Pressure exchanger efficiency	90%
Electric motor efficiency	98%
The cost of electricity [$ (kWh)−1]	0.08
Pressure vessel cost ($)	1000
Seawater intake pump cost (C_{SWIP}), $\$(kg/s^{-1})^{-0.8}$	3.53×10^4
HPP capital cost (C_{HPP}), $\$(kg/s \times MPa)^{-1}$	187
BP capital cost (C_{BP}), $\$(kg/s{\times}MPa)^{-1}$	187
PE capital cost (C_{PE}), $\$(kg/s)^{-0.58}$	6590
Operating cost for pressure vessel (O_{PV}), $(yr.)^{-1}$	0.2
Seawater intake pump operating cost (O_{SWIP}), $\$(kg/s \times yr.)^{-1}$	315
HPP operation cost (O_{HPP}), $\$(kg/s \times MPa \times yr.)^{-1}$	8174
PE operation cost (O_{PE}), $\$(kg/s \times MPa \times yr.)^{-1}$	9082
Insurance operation cost ($O_{INSURANCE}$), $(yr.)^{-1}$	0.063
Labor operation cost (O_{LABOR}), $\$(kg/s \times yr.)^{-1}$	283.8
Chemical usage operation cost ($O_{CHEMICAL}$), $\$(kg/s \times yr.)^{-1}$	638.6
Maintenance operation cost (O_{MAINT}), $\$(kg/s \times yr.)^{-1}$	283.8

Case study one

For the first case study, we explore the production of two permeate streams with different flow rates and TDS concentrations. This is achieved by processing feed seawater stream with relatively high TDS concentration (e.g., 48,000 ppm). In both conditions (with and without permeate splitting), the optimizer selects a single-RO stage to process the seawater feed stream. Figure 9 shows the RO layout with permeate extraction from the pressure vessel; whereas Figure 10 depicts the RO layout without permeate extraction condition for the same case study. Table 3 gives the input and output results for the current case study.

For the first condition (permeate splitting), the total cost of the RO layout is $525,900 per year. The feed seawater is split into the HPP and the PE units, and later combined after a BP as a high-pressure stream to the RO stage. Inside the pressure vessel, there are six extracted permeate streams to the final product permeates. The strict TDS quality (250 ppm) for the second product permeate is satisfied mostly from the front modules, whereas the other product permeate concentration constraint (i.e., TDS is less than 500 ppm) is met from the last two elements. Energy from the high pressure reject stream is recovered in the PE unit.

The other condition (no permeate extraction) has a simpler layout with TAC cost around $576,780 per year. However, the treatment cost is higher than the first condition with 9% cost saving in the case of permeate extraction. There are many essential differences in terms of design and operation of the pressure vessels as a result of permeates extraction condition, Table 3. Higher seawater feed is required in the case of nonexistence of permeate extraction streams with SW30HR-320 as the selected membrane type. Also, the design satisfies exactly the permeate quality constraints in the case of permeate extraction (e.g., 500 ppm for Permeate 1, 250 ppm for Permeate 2). For the other case, both product permeate streams have the permeate quality of 250 ppm of TDS which exceeds the first product permeate requirements.

The stream properties inside the pressure vessels give more insight about the RO design differences, Figures 11 and 12. The pressure drop inside the pressure vessels are almost the same in both conditions, Figure 11. Conversely, the osmotic pressure in the case of permeate extraction is higher than the other condition due to the lower seawater feed stream and higher system recovery (i.e., system recovery around 51.8%). Figure 12 shows the total flux in both conditions with lower values in the case of permeate extraction. The overall permeate recovery in the case of permeate extraction is 51.8 and 42.9% in the other case. To summarize these results, permeate extraction from the RO pressure vessels provide lower cost, higher system recovery, and meet exactly the permeate product specifications.

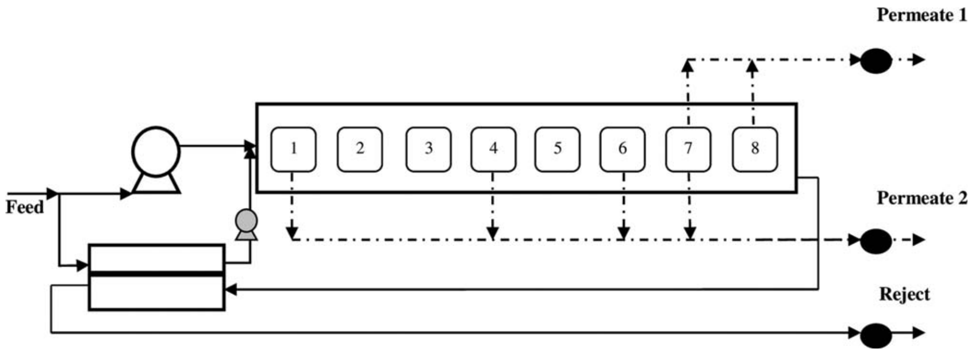

Figure 9. RO layout under permeate splitting condition (Case study one).

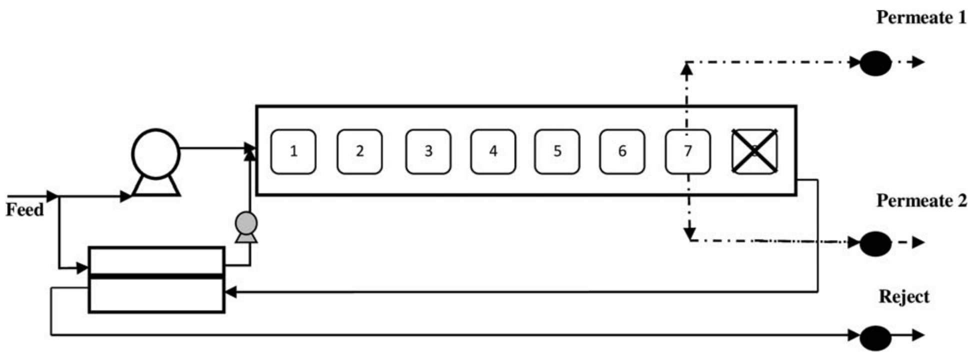

Figure 10. RO layout without permeate splitting condition (Case study one).

Table 3. Input Parameters and Output Results for Case Study One

	Input Data	
Feed seawater salinity (ppm)	48,000	
Permeate 1 demand (kg/s, kg/kg)	25, 5×10^{-4}	
Permeate 2 demand (kg/s^{-1}, kg/kg)	10, 2.5×10^{-4}	
	Output Results	
	With Permeate Splitting	Without Permeate Splitting
# of elements	8	7
# of pressure vessels	26	24
Membrane type	SW30HR-380	SW30HR-320
TAC ($/year)	525,900	576,780
System recovery (%)	51.8	42.9

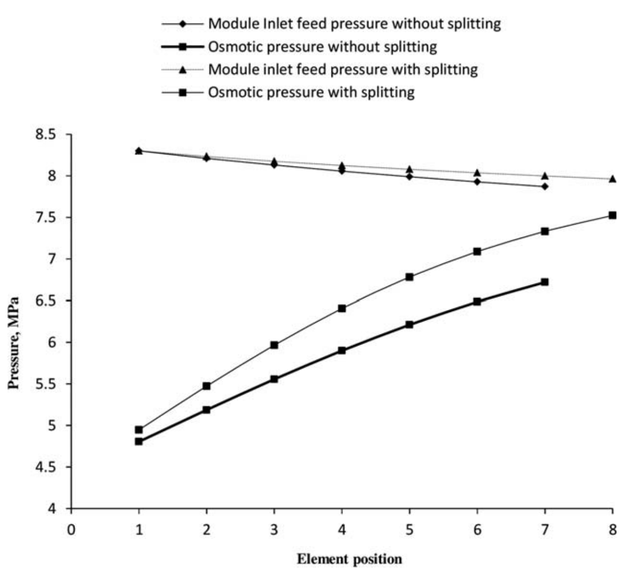

Figure 11. RO feed pressure and osmotic pressure along the pressure vessel length.

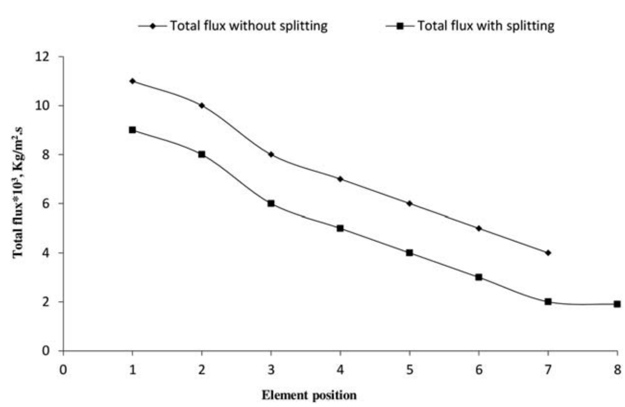

Figure 12. Total flux distribution along the RO pressure vessel length.

Table 4. Input Parameters and Output Results for Case Study Two

Input Data		
Feed seawater salinity (ppm)	30,000	
Permeate 1 demand (kg/s, kg/kg)	25, 5×10^{-4}	
Permeate 2 demand (kg/s, kg/kg)	10, 5×10^{-5}	
Output Results		
	With Permeate Splitting	Without Permeate Splitting
# of elements (Stage 1, Stage 2)	8, 7	7, 8
# of pressure vessels (Stage 1, Stage 2)	22, 7	26, 8
Membrane type (Stage 1, Stage 2)	SW30XLE-400, SW30XLE-400	SW30XLE-400, SW30HR-320
TAC ($/year)	450, 395	461, 479
System recovery (%)	59.2	57.5

Case study two

The second case study investigates the production of two permeate streams with more strict conditions (e.g., 500 ppm, 50 ppm), Table 4. The seawater feed concentration is lower than the first case study (30,000 ppm) which requires two RO stages under permeate splitting and nonsplitting conditions. There is a general similarity of the optimal solutions for both conditions where the first pass treats the seawater feed stream and the second pass treats the first pass permeate stream, Figures 13 and 14.

For the first condition (permeate splitting), the treatment cost is around $450,395 per year with SW30XLE-400 as the membrane type for the first and the second stages. The overall permeate recovery from the system is around 59.2%. The first element in the first pass (e.g., high quality permeates) supplies partially the strict second permeate product stream, whereas the last element delivers the demand for the loose permeate stream. The fifth element delivers the feed stream to the second RO stage. In the second pass, the permeate products from the second pass elements supply the second final permeate product (Permeate 2). In this case study, one can see mixing reject stream from the second pass with the final permeate product stream (Permeate 1) due to the acceptable operation range.

The second condition of this case study does not allow permeate splitting with a treatment cost around $461,479 per year, Figure 14. The membrane type arrangement for the RO passes is SW30XLE400 for the first pass and SW30HR-320 for the second pass. The RO layout for the second condition is similar to the first one in this case study where the first pass treats seawater stream and the second pass treats partially the first pass permeate stream. The reject stream from the second pass supplies minute mass flow rate for the first final permeate product stream. The overall permeate recovery for the second condition is around 57.5%. In this case study, we see that the SPSPRO provides lower cost and higher permeate recovery compared with the nonpermeate splitting condition. However, these differences are not large due to the low TDS seawater feed concentration (30,000 ppm of TDS), Table 4.

Case study three

The current case study presents the problem of two permeate production from seawater stream with 35,000 ppm TDS concentration, Table 5. In this case study, the design requirements show the demand of two permeate streams with different specifications. The first permeate stream has a mass flow rate demand lower than the other one with loose TDS concentration. The solutions for both conditions (with and without permeate splitting) chooses two RO stages to reach the final permeate product specifications, Figures 15 and 16. However, there are essential differences regarding the stream assignments in these conditions with an overall cost saving of 4% if one adopts the permeate splitting condition. The system recoveries are 53% in the case of permeate splitting and 50% in the other case.

For the first condition (permeate splitting), the first stage supplies the final permeate product (Permeate 2 in Figure 15) which has strict requirement around 100 ppm of TDS concentration. The last element supplies the loose permeate

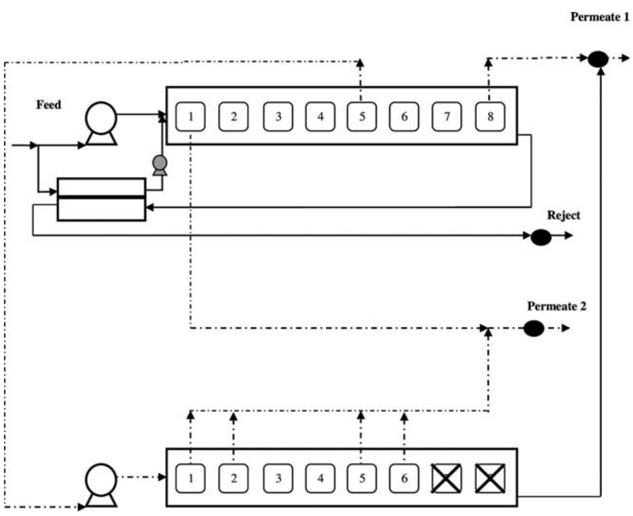

Figure 13. RO layout under permeate splitting condition (Case study two).

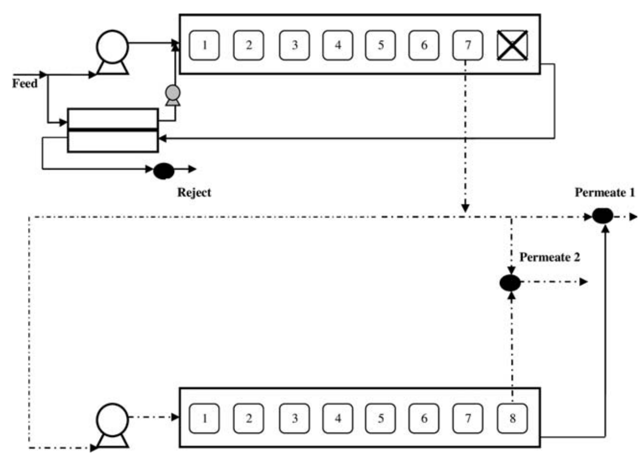

Figure 14. RO layout without permeate splitting condition (Case study two).

Table 5. Input Parameters and Output Results for Case Study Three

	Input Data	
Feed seawater salinity (ppm)	35,000	
Permeate 1 demand (kg/s, kg/kg)	10, 5×10^{-4}	
Permeate 2 demand (kg/s, kg/kg)	25, 1×10^{-4}	
	Output Results	
	With Permeate Splitting	Without Permeate Splitting
# of elements (Stage 1, Stage 2)	6, 5	5, 4
# of pressure vessels (Stage 1, Stage 2)	15, 7	19, 21
Membrane type (Stage 1, Stage 2)	SW30XLE-400, BW30–400	SW30XLE-400, SW30XLE-400
TAC ($/year)	520, 695	543, 296
System recovery (%)	53.5	50.3

product stream with 500 ppm TDS specification. The second stage is solely dedicated to the strict permeate product. This stage processes mainly a permeate stream from the first stage. Again, one can notice mixing the reject stream from the second pass with the loose permeate product (Permeate 1). The membrane type selections are SW30XLE400 and BW30–400 for the first and second passes, respectively. The overall treatment cost with this condition is around $520,695 per year.

The optimal solution for the second condition shows similar layout compared with the first condition. The seawater stream is processed in the first RO pass to deliver the most strict permeate product stream (Permeate 2) and the loose permeate product (Permeate 1), Figure 16. Along the process path, the second pass treats a permeate stream coming from the first stage. In this condition, the overall treatment cost is around $543,296 per year. It should be noted that the membrane type selection is SW30XLE400 for both stages.

Case study four

The current case study presents the production problem of three permeates as final products with different flow rates and TDS requirements, Table 6. The seawater feed stream has 35,000 ppm TDS concentration which must be reduced to the product constraints. The optimal solutions for both conditions (with and without permeate splitting) have two RO stages with permeate processing in the second stage, Figures 17 and 18. The cost saving with permeate splitting condition is around 10%. Besides, the membrane type selections are similar in both conditions.

For the first condition (permeate splitting), the overall treatment cost is $577,471 per year with SW30XLE-400 as the membrane type for the first RO stage. The first stage delivers high quality permeate product from the front modules to the final permeate product which has the most strict TDS concentration constraints (e.g., 140 ppm for Permeate 2 and 60 ppm for Permeate 3). The last RO module supplies the loose final permeate product (Permeate 1). Energy is recovered from the RO reject stream in the first pass. In the second RO stage, the RO permeate products are fully devoted to supply high quality permeates to the final strict permeate product (Permeate 2 and 3). The selected membrane type in this stage is BW30–400. We observe that the reject from the second pass is mixed with the final permeate product stream (Permeate 1). The overall permeate recovery is around 55% in this design condition.

In the second condition (without permeate splitting), the seawater treatment cost is around $638,887 per year with similar membrane type as compared with the first condition. The first RO pass supplies all final permeate products and the second RO stage processes the permeate stream from the first pass to the final strict permeate products (Permeate 2 and 3). In this design, the permeate recovery (48.7%) is less than the first condition which adopts permeate splitting options. In general, it can be concluded that permeate extraction option from the RO pressure vessels provides lower

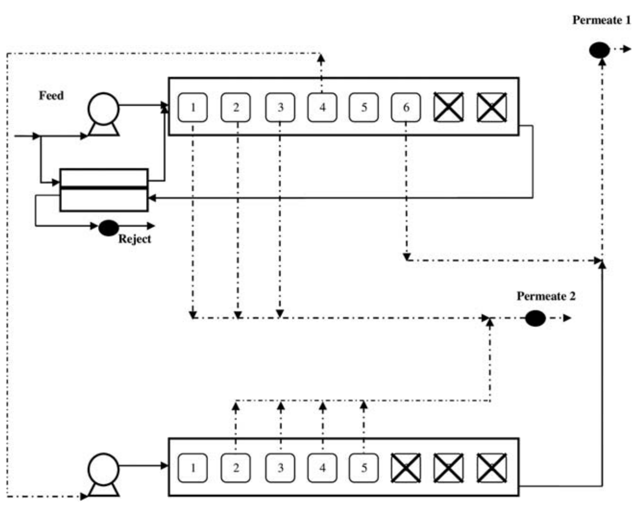

Figure 15. RO layout under permeate splitting condition (Case study three).

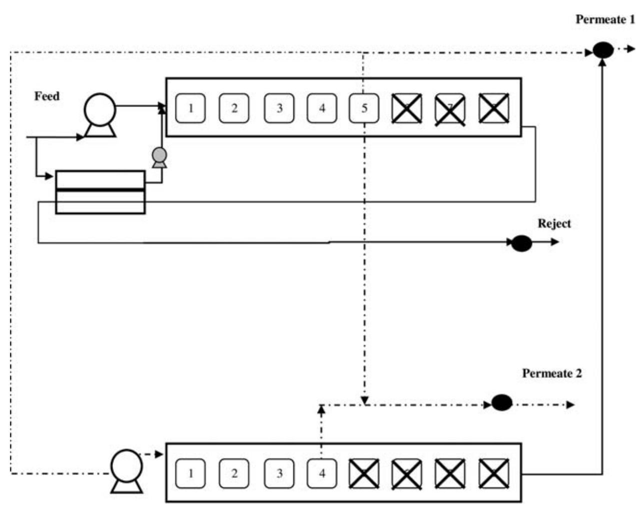

Figure 16. RO layout without permeate splitting condition (Case study three).

Table 6. Input Parameters and Output Results for Case Study Four

Input Data		
Feed seawater salinity (ppm)	35,000	
Permeate 1 demand (kg/s, kg/kg)	25, 5×10^{-4}	
Permeate 2 demand (kg/s, kg/kg)	10, 1.4×10^{-4}	
Permeate 3 demand (kg/s, kg/kg)	8, 6×10^{-5}	
Output Results		
	With Permeate Splitting	Without Permeate Splitting
# of elements (Stage 1, Stage 2)	7, 5	3, 1
# of pressure vessels (Stage 1, Stage 2)	25, 6	55, 60
Membrane type (Stage 1, Stage 2)	SW30XLE-400, BW30–400	SW30XLE-400, BW30–400
TAC ($/year)	577, 471	638, 887
System recovery (%)	55.5	48.7

seawater treatment cost, higher permeate recoveries, and allowance for permeate production with different TDS concentrations.

There are many large scale SPSPRO desalination plants which implement the proposed design concept.[20] The main driver for such design is to achieve very low TDS concentration and to reduce boron concentration in the final products. Boron control requires not only the permeate splitting from the pressure vessels, but also the temperature control inside the pressure vessels.[2] In addition the chemistry of the RO reject stream is an important factor for an effective desalination process (i.e., controlling the pH of the RO reject streams). In our future work, we will extend the proposed mathematical programming model to investigate the optimal SPSPRO network under boron restrictions for the final permeate products. This goal imposes requirements about designing the optimal SPSPRO with heat exchanger network and optimal chemical injection for the streams in the final SPSPRO layout.

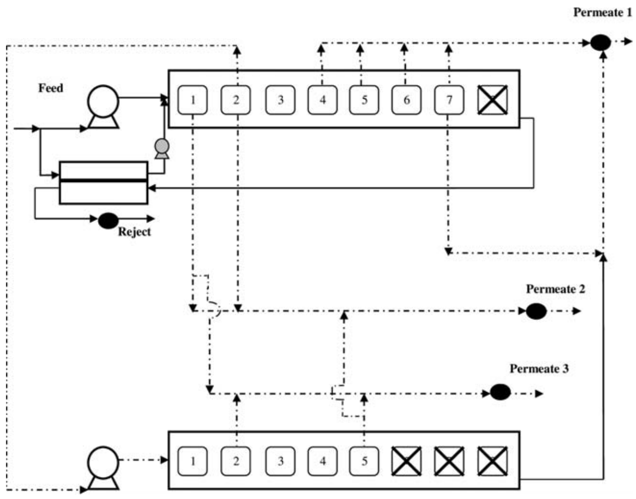

Figure 17. RO layout under permeate splitting condition (Case study four).

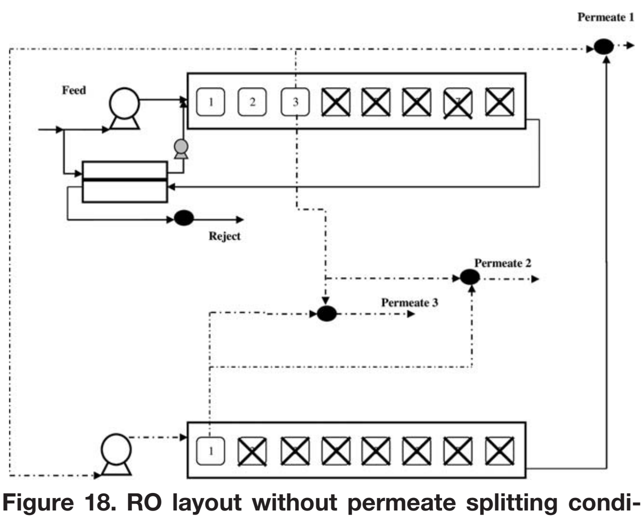

Figure 18. RO layout without permeate splitting condition (Case study four).

Conclusions

In this research study, we presented the SPSPRO design concept for seawater desalination application. Such design concept allows the production of a range of permeate product streams along the RO pressure vessel length. A superstructure is given to represent large process layouts which combine RO pressure vessels in different stages with auxiliary equipments. This graphical representation shows permeate splitting streams from the RO pressure vessels which flow to different RO stages and final permeate products.

A mixed integer nonlinear programming model (MINLP) was consequently developed based on the proposed graphical superstructure that gives rich process layouts. Binary variables allow the selection for RO membrane types, RO membrane modules and stages, and stream assignments in the network. The objective function is to minimize the treatment cost for seawater stream and produce a range of permeate products. The effectiveness of the design concept was verified with several desalination case studies. In general, lower treatment cost with higher permeate recoveries are achieved by allowing permeate splitting streams in the RO design network.

Notation

Abbreviations

DB = distribution box
GAMS = general algebraic modeling system
HPP = high-pressure pump
MINLP = mixed integer nonlinear program
PIF = practical investment factor
RO = reverse osmosis
SPSPRO = split partial second pass reverse osmosis
TAC = total annual cost
TDS = total dissolved salt

Sets

BP = set of booster pumps
Elem = element set in an RO stage

Exit = exit nodes in the DB
HPP = set of high-pressure pumps
Inlet = inlet nodes in the DB
Memb = set of membrane type in every RO module
PE = set of pressure exchangers
PERMEATE = set of final permeate product streams
SRO = set of reverse osmosis stages
SWIP = set of seawater intake pump

Symbols

AOC = annual operation cost ($/year)
AF = annualized factor (1/year)
B = salt permeability coefficient in an RO element (kg/m^2 s)
D = TDS diffusivity in every RO element (m^2/s)
F = mass flow rate of a network stream (kg/s)
k = TDS mass transfer coefficient (m/s)
L = effective length of the RO element (m)
n = exponent in cost functions
NPV = number of the pressure vessels in every RO stage
P = stream pressure (Mpa)
Q = reject volumetric flow (m^3/s)
Re = Reynold's number for every RO element
SA = effective membrane surface area for every RO module (m^2)
Sc = Schmidt number for every RO element
TAC = total annual cost ($/year)
TCC = total capital cost ($)
V = permeate velocity in every RO element (m/s)
W = membrane element width (m)
Wa = water permeability coefficient in an RO element (kg/m^2 Mpa s)
x = TDS concentration (kg/kg)
y = binary variable

Greek letters

ΔP = pressure drop (Mpa)
μ = reject viscosity in every RO element (Kg/m s)
π = osmotic pressure (Mpa)
ρ = stream density (kg/m^3)

Superscripts

Avg = average value in the reject or permeate sides
Bulk = bulk condition at the reject side
f = feed conditions for an RO element
HI = inlet high-pressure stream in a PE unit
In = inlet condition for an RO element
LO = lower bound
Out = outlet condition for an RO element
PERM = designates a property for a permeate stream
P-Wall = conditions at the permeate side membrane wall
Rej = a reject stream property in RO network
R-Wall = conditions at the reject membrane wall
Salt = designates property for salt
UP = upper bound
Wat = designates a property for pure water
WITHD = represents property for withdraw permeate stream

Literature Cited

1. Fritzmann C, Löwenberg J, Wintgens T, Melin T. State-of-the art of reverse osmosis desalination. *Desalination*. 2007;216:1−76.
2. Rybar S, Boda R, Bartels C. Split partial second pass design for SWRO plants. *Desalination Water Treat*. 2010;13:186–194.
3. Evangelista F. Explicit expressions for permeate flux and concentration in hyperfiltration. *Chem Eng Sci*. 1986;41:1913.
4. Papafotiou K, Assimacopoulos D, Maroulis-Kouris D. A knowledge based system for the design of RO-desalination plants, desalination and water re-use. *Proceedings of the 12th International Symposium*. Rugby, UK: IchemE, 1991.
5. El-Halwagi MM. Optimal design of membrane-hybrid systems for waste reduction. *Sep Sci Technol*. 1993;28:283–307.
6. Lutze P, Gani R, Woodley JM. Process intensification: a perspective on process synthesis. *Chem Eng Process*. 2010;49:547–558.
7. Saif Y, Elkamel A, Pritzker M. Superstructure optimization for the synthesis of chemical process flowsheets: application to optimal hybrid membrane systems. *Eng Optim*. 2009;41:327–350.
8. El-Halwagi MM. Synthesis of reverse osmosis networks for waste reduction. *AIChE J*. 1992;38:1185–1198.
9. Alnouri S, Linke P. A systematic approach to optimal membrane network synthesis for seawater desalination. *J Memb Sci*. 2012;417: 96–112.
10. Saif Y, Elkamel A, Pritzker M. Optimal design of reverse-osmosis network for wastewater treatment. *Chem Eng Proc*. 2008;47:2163–2174.
11. Saif Y, Elkamel A, Pritzker M. Global optimization of reverse osmosis network for wastewater treatment and minimization. *Ind Eng Chem Res*. 2008;47:3060–3070.
12. Maskan F, Wiley DE, Johnston LPM, Clements DJ. Optimal design of reverse osmosis module networks. *AIChE J*. 2000;46:946–954.
13. Du Y, Xie L, Wang Y, Xu Y, Shichang W. Optimization of reverse osmosis networks with spiral wound modules. *Ind Eng Chem Res*. 2012;51:11764–11777.
14. Lu YY, Hu YD, Zhang XL, Wu LY, Liu QZ. Optimum design of reverse osmosis system under different feed concentration and product specification. *J Memb Sci*. 2007;287:219−229.
15. Lu Y, Hu Y, Xu D, Wu L. Optimum design of reverse osmosis seawater desalination system considering membrane cleaning and replacing. *J Memb Sci*. 2006;282:7–13.
16. See HJ, Vassiliadis VS, Wilson DI. Optimization of membrane regeneration scheduling in reverse osmosis networks for seawater desalination. *Desalination*. 1999;125:37–54.
17. Zhu M, El-Halwagi MM, Al-Ahmad M. Optimal design and scheduling of flexible reverse osmosis networks. *J Memb Sci*. 1997;129: 161–174.
18. Bartels C, Cioffi S, Rybar S, Wilf M, Koutsakos E. Long term experience with membrane performance at the Larnaca desalination plant. *Desalination*. 2008;221:92–100.
19. Bray DT. US Patent 4,046,685. 1977.
20. Peñate B, García-Rodríguez L. Current trends and future prospects in the design of seawater reverse osmosis desalination technology. *Desalination*. 2011;284:1–8.
21. Mussati S, Aguirre P, Scenna NJ. Superstructure of alternative configurations of the multistage flash desalination process. *Ind Eng Chem Res*. 2006;45:7190–7203.
22. Kraemer K, Kossack S, Marquardt W. Efficient optimization based design of distillation processes for homogeneous azeotropic mixtures. *Ind Eng Chem Res*. 2009;48:6749–6764.
23. Grossmann IE, Aguirre PA, Barttfeld M. Optimal synthesis of complex distillation columns using rigorous models. *Comput Chem Eng*. 2005;29:1203–1215.
24. Geraldes V, Pereira NE, Pinho MN. Simulation and optimization of medium-sized seawater reverse osmosis processes with spiral wound Modules. *Ind Eng Chem Res*. 2005;44:1897–1905.
25. Kaghazchi T, Mehri M, Ravanchi M, Kargari A. A mathematical modeling of two industrial seawater desalination plants in the Persian Gulf region. *Desalination*. 2010;252:135–142.
26. Hyung H, Kim JH. A mechanistic study on boron rejection by seawater reverse osmosis membranes. *J Memb Sci*. 2006;286:269–278.
27. Malek A, Hawlader MNA, Ho JC. Design and economics of RO seawater desalination. *Desalination*. 1996;105:245–261.
28. Viswanathan J, Grossmann IE. A combined penalty function and outer approximation method for MINLP optimization. *Comput Chem Eng*. 1990;14:769–782.
29. Brooke A, Kendrik D, Meeraus A. *GAMS User's Guide*. Danvers, MA: Boyd & Fraser Publishing Co, 1992.
30. Duran M, Grossmann. An outer-approximation algorithm for a class of mixed-integer nonlinear programs. *Math Program*. 1986;36:307–339.

Manuscript received Mar. 22, 2013, and revision received Oct. 5, 2013.